

# An ML-Driven Participant Selection Technique for Federated Recommendation System in Edge-Cloud Computing

Jintao Liu<sup>1</sup>, Mohammad Goudarzi<sup>1</sup>, and Adel Nadjaran Toosi<sup>2</sup>

<sup>1</sup>The Faculty of Information Technology, Monash University, Australia

<sup>2</sup>School of Computing and Information Systems, The University of Melbourne, Australia

**Abstract**—Recommendation systems (RS) personalize content by analyzing user preferences, but typically require centralized collection of user data, raising privacy and scalability concerns. Federated Recommendation Systems (FRS) address these issues by enabling distributed, privacy-preserving model training across edge devices, keeping raw data on-device. Although existing FRS frameworks benefit from on-device feature extraction and privacy preservation, they suffer from heterogeneous device capabilities, non-independent and identically distributed (non-IID) data, and communication bottlenecks. To overcome these limitations, we propose a multi-objective reinforcement learning (RL) participant selection that jointly optimizes historical client performance reputation (CPR), data utility, and system efficiency. First, we define a composite client-utility function combining CPR, system capability, and data quality. Next, we embed this utility into a multi-armed bandit (MAB) framework and dynamically balance exploration–exploitation to select participants. Finally, we practically implement our approach using the PySyft framework on an edge–cloud testbed, and evaluate it on a multimodal movie-recommendation task built from the MovieLens-100K dataset. Across four different skewed data-partition scenarios, our MAB-based selection accelerates convergence by 32–50% in time-to-target AUC and reduces total wall-clock training time by up to 46%, while matching or slightly improving final AUC, NDCG@50, and Recall@50 compared to existing FRS baselines. Our results demonstrate that adaptive, reward-driven client sampling can substantially enhance both efficiency and fairness in real-world federated deployments.

**Index Terms**—Federated recommendation systems, multi-armed bandit, participant selection, reinforcement learning

## I. INTRODUCTION

With the ongoing information explosion, users are provided with an exponentially growing scale of digital content, exemplified by Amazon’s 2024 catalog exceeding 353 million products [1] and TikTok’s 8.6 billion video uploads [2]. At this scale, manual discovery of user interests becomes impractical, necessitating the widespread adoption of RS to discern user preferences and facilitate decision-making.

Traditionally, RS have followed a cloud-centric paradigm: service providers collect user–item interactions, profiles, and auxiliary data to train models on powerful central servers [3]. Early methods relied on matrix factorization (MF) to decompose interaction matrices into latent factors; however, they are not suitable to handle complex behaviors. The advent of deep neural networks has enabled capturing nonlinear patterns more effectively, further exploiting higher-order user–item relationships and yielding significant accuracy

gains [4].

Although cloud-based RS achieve high accuracy by leveraging large-scale interaction data, they struggle to accommodate the growing diversity and volume of multimodal user signals (i.e., textual reviews, images, audio clips, and videos) without incurring latency, bandwidth consumption, and privacy risks [5]. Also, despite impressive progress, centralized RS with cloud-based approaches inherently demand the continuous collection and storage of sensitive personal data. Such concentration of information not only heightens the exposure to large-scale breaches but also conflicts with an evolving landscape of privacy legislation [6]. Regulatory frameworks like the European Union’s General Data Protection Regulation (GDPR) [7] and China’s Personal Information Protection Law (PIPL) [8] underscore a global shift toward user data sovereignty, enforcing strict controls on how personal information may be gathered, processed, and transferred. These mandates present a profound challenge for centralized RS.

Edge–cloud architectures address these challenges by partitioning the recommendation pipeline: lightweight models deployed at the network edge extract features and perform preliminary inference on raw multimodal inputs, while the cloud aggregates the full spectrum of user data to train and update the global models [9], [10]. As for privacy concerns, federated learning (FL) among distributed edge–cloud computing nodes emerges as an alternative paradigm, enabling collaborative model training without sharing raw data. By keeping user interactions on-device and sharing only aggregated updates, this paradigm offers a principled path to strong privacy guarantees [6]. However, deploying FRS in a practical edge–cloud computing environment entails its own set of challenges due to common challenges in distributed scheduling [11]: heterogeneous hardware settings, non-IID data across devices, communication bottlenecks [10], and the difficulty of balancing data skew in global aggregation especially with multi-modality data [12]. To overcome these challenges and improve the efficiency of FL, the process of participant selection among heterogeneous clients is of paramount importance.

In FL systems, participant selection strategies are broadly categorized into two approaches: data utility maximization and system utility optimization [13]. Data utility maximization strategies employ importance-based ranking mechanisms that leverage various metrics including gradient norm, local

loss [13], Shapley value [14], and CPR [15] to identify the most valuable participants. These approaches are complemented by clustering-driven methodologies such as hierarchical grouping and K-means clustering to organize clients based on data characteristics. System utility optimization strategies utilize optimization techniques to achieve optimal trade-offs between global model objectives and practical constraints such as bandwidth limitations and computational resources [16]. Additionally, RL frameworks enable dynamic exploration-exploitation trade-offs during client sampling [17], [18], while advanced hybrid frameworks integrate multiple selection criteria through two-stage utility optimization combined with deep reinforcement learning (DRL) methodologies [13], [19].

Despite the theoretical advances in participant selection strategies, their practical implementation in FRS remains significantly limited due to the complex interplay of device heterogeneity, availability constraints, and diverse data characteristics. Current FRS research predominantly focuses on global model optimization within simulated environments that do not adequately represent actual computing device constraints and capabilities. The existing literature can be categorized into three main research directions: security-oriented approaches that utilize local differential privacy and clustering methods to detect malicious nodes and free-riders [20], [21], [22], [23], fairness-focused studies that address equitable participation in the FL process [24], [25], and heterogeneity-aware solutions that tackle challenges including cross-silo data integration from different organizations and cold start problems in recommendation scenarios [26], [27], [28].

To address both system and data heterogeneity in practical multi-modal FRS, we employ an adaptive MAB-based RL strategy that prioritizes clients optimizing both data and system utilities, and we cast the dynamic client sampling problem into a non-stationary MAB framework. By treating each client as an arm, the MAB formulation naturally balances exploration with discovering under-sampled clients and exploitation within selecting clients with proven high utility. This principled approach adapts to fluctuating device capabilities, communication constraints, and non-IID data distributions, directly mitigating the challenges of skewed data, heterogeneous hardware, and communication bottlenecks in federated recommendation.

- 1) We introduce a unified utility optimization formulation that integrates historical CPR, system efficiency, and data quality into RL reward, enabling dynamic trade-offs between accuracy, efficiency, and fairness.
- 2) We propose a MAB-based selection algorithm that learns optimal exploration-exploitation policies in non-stationary federated environments, improving training efficiency and fairness under client heterogeneity.
- 3) We implement and evaluate our method in the practical edge-cloud FL settings for the movie recommendation task, demonstrating a 32%–50% improvement in time-to-target AUC across four data distributions while matching state-of-the-art final performance.

The rest of this paper is organized as follows. Section II provides background on multi-modality RS, FL, and participant selection strategies. Section III presents our system model, multi-objective optimization goal and formalizes the participant selection problem. Section IV details the RL formulation and the proposed MAB selection algorithm. Section V describes the experimental setup and reports numerical results on the MovieLens-100K dataset. Section VI discusses ethics and data privacy considerations. Finally, Section VII concludes the paper and outlines future work.

## II. BACKGROUND

This section provides an overview of three topics: Multi-Modality RS, FL, and Participant Selection Strategies. Finally, related works for participant selection in FRS are described in this section.

### A. Multi-Modality Recommendation System

Model-based collaborative filtering (CF) methods project users and items into a shared latent space, where interactions are predicted via similarity functions. Early successes include MF techniques, which minimize the reconstruction error of the user-item matrix, and probabilistic extensions such as Probabilistic Matrix Factorization (PMF) [3]. To better capture non-linear interactions, Neural Collaborative Filtering (NCF) replaces the inner product with multi-layer perceptrons [29]. However, these methods often underperform in sparse regimes or cold-start scenarios, since they rely exclusively on interaction histories.

To alleviate sparsity, auxiliary content such as textual reviews and visual features have been fused with CF. Visual Bayesian Personalized Ranking (VBPR) injects pretrained image embeddings into the ranking objective [30]. However, fusing heterogeneous modalities remains challenging due to distributional mismatch and complementary information gaps. Disentangled multimodal representation learning (DMRL) disentangles fine-grained text and image factors to better model item characteristics [31].

As shown in Figure 1, we evaluate the performance of the models on the widely used MovieLens-100K benchmark [32], using Precision, Recall, NDCG, F1, and AUC (see Section V-D.1 for detailed definitions) to assess the effectiveness of each model. As evidenced in the figure, the multi-modality RS model consistently achieves the highest values across all evaluation metrics. Specifically, DMRL attains an AUC of 0.9219, an F1@50 of 0.1856, and an NDCG@50 of 0.3241. This advantage arises because multi-modality RS can learn richer, complementary feature representations by jointly leveraging heterogeneous data sources—such as collaborative signals, textual metadata, and visual item features.

### B. Federated Learning

FL is a decentralized training paradigm in which a central server orchestrates model updates across a large number of clients that each retain their data locally. In every communication round, the server sends the current global model parameters to a selected group of clients [12]. These clients

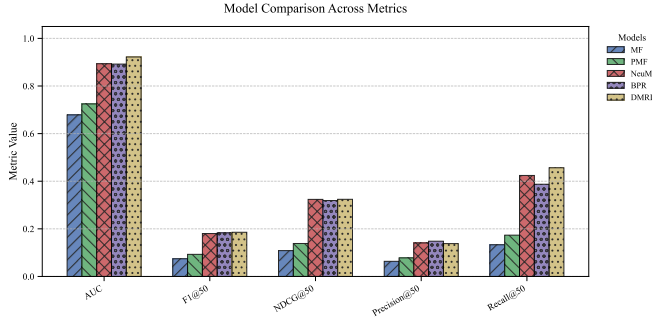


Fig. 1: Model Evaluation over Recommendation Metrics

then perform several epochs of local optimization on their own datasets and return only their model updates or gradients. When the server aggregates these updates, usually by weighting them according to the size of each client’s dataset, it produces an improved global model without ever accessing raw data. This iterative process continues until the model converges, enabling collaborative learning while preserving user privacy [6].

Deploying FL at scale introduces several practical challenges. First, non-IID distributed data across clients can bias local updates and slow convergence. Second, constrained bandwidth and unreliable network connections can delay or disrupt synchronization. Third, a heterogeneous distribution of computational resources may give rise to straggler problems and induce training delays [12]. To mitigate these issues, adaptive aggregation methods can be used to adjust each client’s contribution based on criteria such as data volume and the recency of updates [33]. Moreover, intelligent participant selection is essential: by choosing clients with diverse data profiles or sufficient computational resources, the system can improve training efficiency, ensure fair representation, and ultimately enhance overall model quality [13].

### C. Related Work

Recent studies in FL and FRS have explored critical challenges across different dimensions: asynchronous FL, data heterogeneity, system heterogeneity, participant selection, privacy, and personalization.

1) *Asynchronous FL*: While most FL frameworks assume synchronous updates, straggler clients often degrade system efficiency. Asynchronous FL addresses this by enabling clients to participate at flexible intervals. In FRS, Imran *et al.* [34] proposed an asynchronous clustering-based framework that adapts to dynamic user preferences. Beyond FRS, Flight has been introduced to support containerized orchestration, leveraging the mature FogBus2 edge-cloud computing framework [35], [36]. Additional advancements include UAV-specific deployments aimed at accelerating convergence [37], and semi-asynchronous models that mitigate aggregation frequency imbalance through predictive scheduling [38].

2) *Cross-Silo Heterogeneity*: Cross-silo scenarios introduce data inconsistency and cold-start issues. Li *et al.* [27] proposed a privacy-preserving FRS framework using

cryptographic protocols to address inter-organizational silos while supporting new user recommendations. Alternatively, a multi-modal approach [20] adopts attention mechanisms in asynchronous training to improve flexibility and accuracy. More recently, Zhang *et al.* [39] integrated foundation models and FL using low-rank adapters, reducing both computation and communication costs in personalized environments.

3) *Cross-System Heterogeneity*: System-level heterogeneity arises from variations in client capabilities. HeteFedRec addressed system heterogeneity by enabling clients to train personalized models in different sizes and applying knowledge distillation to reduce bandwidth load [40]. In a real-world advertising setting, Bian *et al.* [41] deployed a cross-platform FRS to serve over 100 million users, improving installation conversion rates and demonstrating practical scalability.

4) *Privacy Preservation*: To balance privacy with resource constraints, Yang *et al.* [42] introduced personalized privacy control using discrete hashing and memory caching. Another framework in Blockchain-based FL ensures traceability and privacy without degrading performance [43], while Ding *et al.* [44] proposed a meta-learning-based aggregation strategy with an item-similarity model to enhance both privacy and training efficiency.

5) *Personalization*: Personalization in FL aims to address client-level data heterogeneity. In Point-of-Interest recommendations, Ye *et al.* [45] introduced adaptive clustering to enhance internal client correlation and statistical alignment, achieving a balance between global model sharing and local personalization.

6) *Participant Selection*: In our specific area of focus on FRS, participant selection refers to the process by which the server chooses a subset of clients to contribute updates at each communication round. Formally, let  $\mathcal{C}$  be the full set of  $K$  clients and  $\mathcal{S}_t \subseteq \mathcal{C}$  the clients selected at round  $t$ . The choice of  $\mathcal{S}_t$  directly impacts convergence speed, model quality, and fairness across heterogeneous clients [46].

In recent studies, Yuan *et al.* [40] proposed HeteFedRec, a federated framework supporting heterogeneous model selection and aggregation mechanism. Xia *et al.* [47] introduced AeroRec, an on-device FRS employing federated self-supervised distillation and selection to boost lightweight-model performance. Feng *et al.* [20] designed a privacy-preserving multimodal RS with clustering-based participant selection to optimize statistical resilience. Li *et al.* [48] presented FedRAP, which learns and selects additive global and personalized item embeddings with sparse regularization for communication efficiency. Li *et al.* [49] proposed FedConPE, a federated conversational bandits algorithm optimizing communication and regret. He *et al.* [50] proposed CoFedRec, a co-clustering mechanism grouping clients and items based on network structure and embedding similarity. Ting *et al.* [51] introduced PriFedRec, which integrates homomorphic encryption for privacy and evaluates client availability and communication delay when selecting participants, demonstrating reduced convergence time.

In summary, common participant selection strategies can

TABLE I: A Comparative Analysis of Participant Selection Approaches in FRS

Method	Data/System Heterogeneity				
	Mode	Data Distri.	Comm. Delay	Comput. Capacity	CPR
RPFL [20]	Simulated	✓	✗	✗	✗
HeteFedRec [40]	Simulated	✓	✗	✓	✗
AeroRec [47]	Simulated	✓	✓	✗	✗
FedRAP [48]	Simulated	✓	✓	✗	✗
FedConPE [49]	Simulated	✓	✓	✓	✗
CoFedRec [50]	Simulated	✓	✗	✗	✗
PriFedRec [51]	Simulated	✓	✗	✗	✗
FedAvg [52]	Simulated	✗	✗	✗	✗
Our Method	Practical	✓	✓	✓	✓

be classified into the following categories:

- 1) **Random Selection:** Each round, a fixed number  $S$  of clients is chosen uniformly at random. This simple approach guarantees unbiased participation in expectation but may repeatedly choose clients with poor connectivity or small data, delaying the convergence in the global model [52].
- 2) **Data-Aware Selection:** Clients whose local gradients have higher variance or whose data distributions differ more from the global distribution may be sampled more frequently to accelerate convergence [20], [40], [47], [48], [49], [50], [51].
- 3) **Resource-Aware Selection:** Client sampling is guided by availability, communication bandwidth, and computational capacity. By prioritizing clients, this approach mitigates straggler effects and reduces overall training latency [40], [47], [48], [49].

Table I summarizes how previous works compare with respect to these selection criteria.

### III. SYSTEM MODEL AND PROBLEM FORMULATION

In this section, we first define a multi-modal RS model with ID, text, and visual embeddings, factor-wise attention, and a unified scoring function. We then introduce client utility optimization formulation with CPR, system quality, and data quality, and incorporate per-round latency into a normalized time model. Finally, we formalize participant selection as an optimization that maximizes aggregate utility under delay constraints.

#### A. Multimodal Recommendation System Model

Let  $\mathcal{U}$  and  $\mathcal{I}$  denote the sets of users and items, with  $|\mathcal{U}| = M$  and  $|\mathcal{I}| = N$ . Each user  $u \in \mathcal{U}$  assigns an explicit rating  $r_{u,i} \in [1, 5]$  to item  $i \in \mathcal{I}$  in the Movielens-100K dataset [32]. For each observed positive pair  $(u, i^+)$ , we uniformly sample  $K$  negatives  $\{i_1^-, \dots, i_K^-\}$  from items not rated by  $u$ . Every item  $i$  is represented by three raw modalities inspired by DMRL [31]:

$$\mathbf{v}_i \in \mathbb{R}^d, \quad \mathbf{t}_i \in \mathbb{R}^{d_T}, \quad \mathbf{x}_i \in \mathbb{R}^{d_V} \quad (1)$$

corresponding to an ID embedding, BERT-derived text features [53], and ViT-derived image features [54], respectively.

We assume  $F$  latent factors (e.g., story, visuals) and set the per-factor dimension  $d_f = d/F$ .

**Embedding Modules:** User and item lookups are implemented as learnable embeddings:

$$\mathbf{p}_u = \text{Embed}_u(u) \in \mathbb{R}^d, \quad \mathbf{v}_i = \text{Embed}_i(i) \in \mathbb{R}^d, \quad (2)$$

where  $\text{Embed}_u, \text{Embed}_i \in \mathbb{R}^{d \times M}$  (resp.  $d \times N$ ) are parameter matrices. Raw text and image features are each projected by a two-layer multilayer perceptron (MLP) with LeakyReLU activations:

$$\begin{aligned} \mathbf{t}'_i &= \text{LReLU}(W_{T,2} \text{LReLU}(W_{T,1} \mathbf{t}_i + b_{T,1}) + b_{T,2}), \\ \mathbf{x}'_i &= \text{LReLU}(W_{V,2} \text{LReLU}(W_{V,1} \mathbf{x}_i + b_{V,1}) + b_{V,2}), \end{aligned} \quad (3)$$

where  $W_{T,1} \in \mathbb{R}^{H_T \times d_T}$ ,  $W_{T,2} \in \mathbb{R}^{d \times H_T}$  (and analogously  $W_{V,1}, W_{V,2}$ ) with biases  $b_{T,1}, b_{T,2}, b_{V,1}, b_{V,2}$ , and dropout rate  $\delta$ .

**Factor-Wise Decomposition:** Each  $d$ -dimensional embedding is partitioned into  $F$  blocks of dimension  $d_f$ :

$$\mathbf{p}_u = [\mathbf{p}_u^{(1)}; \dots; \mathbf{p}_u^{(F)}], \quad \mathbf{v}_i = [\mathbf{v}_i^{(1)}; \dots; \mathbf{v}_i^{(F)}], \quad (4)$$

and similarly  $\mathbf{t}'_i = [\mathbf{t}'_i^{(1)}; \dots; \mathbf{t}'_i^{(F)}]$ ,  $\mathbf{x}'_i = [\mathbf{x}'_i^{(1)}; \dots; \mathbf{x}'_i^{(F)}]$ . For factor  $f$ , we form the concatenated vector

$$\mathbf{h}_{u,i}^{(f)} = [\mathbf{p}_u^{(f)}; \mathbf{v}_i^{(f)}; \mathbf{t}'_i^{(f)}; \mathbf{x}'_i^{(f)}] \in \mathbb{R}^{4d_f}. \quad (5)$$

**Multimodal Attention:** An MLP-based attention mechanism produces normalized weights over the four modality channels for each factor:

$$\alpha_{u,i}^{(f)} = \text{Softmax}\left(A_2 \tanh(A_1 \mathbf{h}_{u,i}^{(f)} + b_1) + b_2\right), \quad (6)$$

where  $A_1 \in \mathbb{R}^{H_a \times 4d_f}$ ,  $A_2 \in \mathbb{R}^{4 \times H_a}$ , and  $b_1 \in \mathbb{R}^{H_a}$ ,  $b_2 \in \mathbb{R}^4$ .

**Scoring Function:** For each factor  $f$ , we weight the user-item interactions across modalities and apply a GELU activation:

$$s_{u,i}^{(f)} = \sum_{s \in \{\text{ID}, T, V\}} \alpha_{u,i,s}^{(f)} \text{GELU}(\langle \mathbf{p}_u^{(f)}, \mathbf{e}_i^{(s,f)} \rangle), \quad (7)$$

with  $\langle \cdot, \cdot \rangle$  denoting the dot product and  $\mathbf{e}_i^{(\text{ID},f)} = \mathbf{v}_i^{(f)}$ ,  $\mathbf{e}_i^{(T,f)} = \mathbf{t}'_i^{(f)}$ ,  $\mathbf{e}_i^{(V,f)} = \mathbf{x}'_i^{(f)}$ . The overall predicted rating is

$$\hat{r}_{u,i} = \sum_{f=1}^F s_{u,i}^{(f)}. \quad (8)$$

**Loss and Regularization:** We train using a pairwise ranking loss that enforces  $s_{u,i^+} > s_{u,i^-}$  by a margin for each sampled negative, promoting higher scores for true positives. To encourage disentanglement among factor embeddings, we add a distance-correlation regularizer that penalizes statistical dependence between any two factor blocks within the same modality. Finally, standard  $L_2$  weight decay is applied to all parameters, and optimization is performed with the AdamW optimizer.



## B. Problem Formulation

The aim of this paper is to select a subset of client nodes in each FL round that maximizes collective contribution while respecting system latency constraints. To this end, we utilize a modular, three-component scoring scheme for each node  $i$ : (i) a customized CPR, (ii) an update relevance measure, and (iii) a data quality metric. These elements are combined into an aggregate contribution score and balanced against expected round time to yield the optimal selection.

1) *Customized Client Performance Reputation*: First, we capture each node's historical effect on global model accuracy via a customized performance reputation. Let  $Q_t^i$  be the validation accuracy contributed by node  $i$  at round  $t$ , and let  $Q_{t-1}$  denote the previous global model accuracy. We update a cumulative reputation  $R_t^i$  according to

$$R_t^i = \gamma \Delta_t^i + (1 - \gamma) R_{t-1}^i, \quad \Delta_t^i = Q_t^i - Q_{t-1}, \quad (9)$$

where  $\gamma \in [0, 1]$  controls the trade-off between the most recent accuracy gain  $\Delta_t^i$  and the historical reputation  $R_{t-1}^i$ . Initializing  $R_0^i$  to zero ensures neutrality at the outset. This exponential smoothing approach rewards nodes that consistently drive improvements while discounting occasional aberrations, providing a stable yet responsive performance indicator.

2) *Update Relevance*: Beyond reputation, we assess how each local model update  $w_t^i$  aligns with the global model  $w_t$ . We quantify the average absolute deviation as follows:

$$\delta_t^i = \frac{1}{d} \sum_{j=1}^d |w_t^{i,j} - w_t^j|, \quad (10)$$

and define the round-specific relevance score as:

$$U_t^i = \begin{cases} \exp(-\delta_t^i), & \text{if } Q_t > Q_{t-1}, \\ 1 - \exp(-\delta_t^i), & \text{otherwise.} \end{cases} \quad (11)$$

When the global model improves ( $Q_t > Q_{t-1}$ ), nodes whose updates lie close to the current global weights are up-weighted via the exponential kernel, thereby favoring consistent directions of improvement. Conversely, if the global accuracy stagnates or degrades, larger deviations are penalized, discouraging noisy or adversarial contributions.

3) *Data Quality Measure*: To reflect the intrinsic value of each node's local dataset, we introduce a data utility metric  $D_i$ :

$$D_i = |B_i| \sqrt{\frac{1}{|B_i|} \sum_{k \in B_i} \ell_k^2}, \quad (12)$$

where  $|B_i|$  is the number of local samples and  $\ell_k$  is the training loss on sample  $k$ . Intuitively,  $D_i$  grows both with dataset size and aggregate loss magnitude, reflecting the potential informativeness of under-fit or diverse samples. We then apply Min-Max normalization to obtain  $\tilde{D}_i \in [0, 1]$ , ensuring comparability across heterogeneous clients.

4) *Aggregate Contribution Score*: Combining the three components yields node  $i$ 's overall score at round  $t$ :

$$S_t^i = \alpha (U_t^i R_t^i) + \beta \tilde{D}_i, \quad (13)$$

where  $\alpha, \beta > 0$  balance the joint update relevance-reputation term against normalized data quality. By tuning  $\alpha$  and  $\beta$ , the coordinator can prioritize trustworthy, performance-proven clients or those possessing valuable data.

5) *Round Time Calculation*: In practical FL deployments, round duration is constrained by the slowest selected participant. Denote the set of chosen nodes by  $N_{\text{sel}}$ . For any node  $n \in N_{\text{sel}}$ , let  $s_n$  be its computation speed,  $d_n$  the communication payload size, and  $b_n$  its available bandwidth. Then

$$T_{\text{round}} = \max_{n \in N_{\text{sel}}} \left( \underbrace{\frac{\sum_{i \in I} n_i}{s_n}}_{\text{compute time}} + \underbrace{\frac{d_n}{b_n}}_{\text{comm. time}} \right), \quad (14)$$

where  $\sum_{i \in I} n_i$  represents the aggregate workload allocated to node  $n$ . Modeling both computation and communication delays ensures robust scheduling under heterogeneous resource profiles.

6) *Normalized Time Usage*: To enforce semi-asynchronous progress, a time boundary  $T_{\text{semi}}$  is imposed. We thus define normalized usage

$$\tilde{T} = \frac{T_{\text{round}}}{T_{\text{semi}}}, \quad (15)$$

capturing the relative latency per round and enabling direct comparison with contribution scores.

7) *Optimal Selection via Joint Optimization*: Finally, the ideal participant subset  $\mathcal{N}_{\text{sel}}$  solves

$$\max_{\mathcal{N}_{\text{sel}} \subseteq \mathcal{N}} \left\{ \sum_{i \in \mathcal{N}_{\text{sel}}} S_t^i - \kappa \tilde{T} \right\}, \quad (16)$$

where  $\kappa > 0$  trades off aggregate model contribution against latency penalty. This combinatorial program can be approached via greedy heuristics or integer programming to identify a near-optimal balance between accuracy gains and time efficiency.

Solving the above selection exactly is NP-hard when  $|\mathcal{N}|$  is large. In practice, a simple greedy algorithm that iteratively adds the client with highest marginal  $S_t^i - \kappa \delta \tilde{T}$  until the time budget is exhausted yields a near-optimal solution in  $O(N \log N)$  time. For moderate-sized systems, one may employ dynamic programming or branch-and-bound to further tighten optimality gaps. Moreover, fairness constraints such as minimum or maximum participation quotas can be incorporated by adding linear constraints to the integer program.

To adapt to evolving network conditions, the hyper-parameters  $\gamma, \alpha, \beta, \kappa$  may themselves be tuned online via Bayesian optimization or heuristic schemes, thus aligning selection behavior with long-term system objectives.

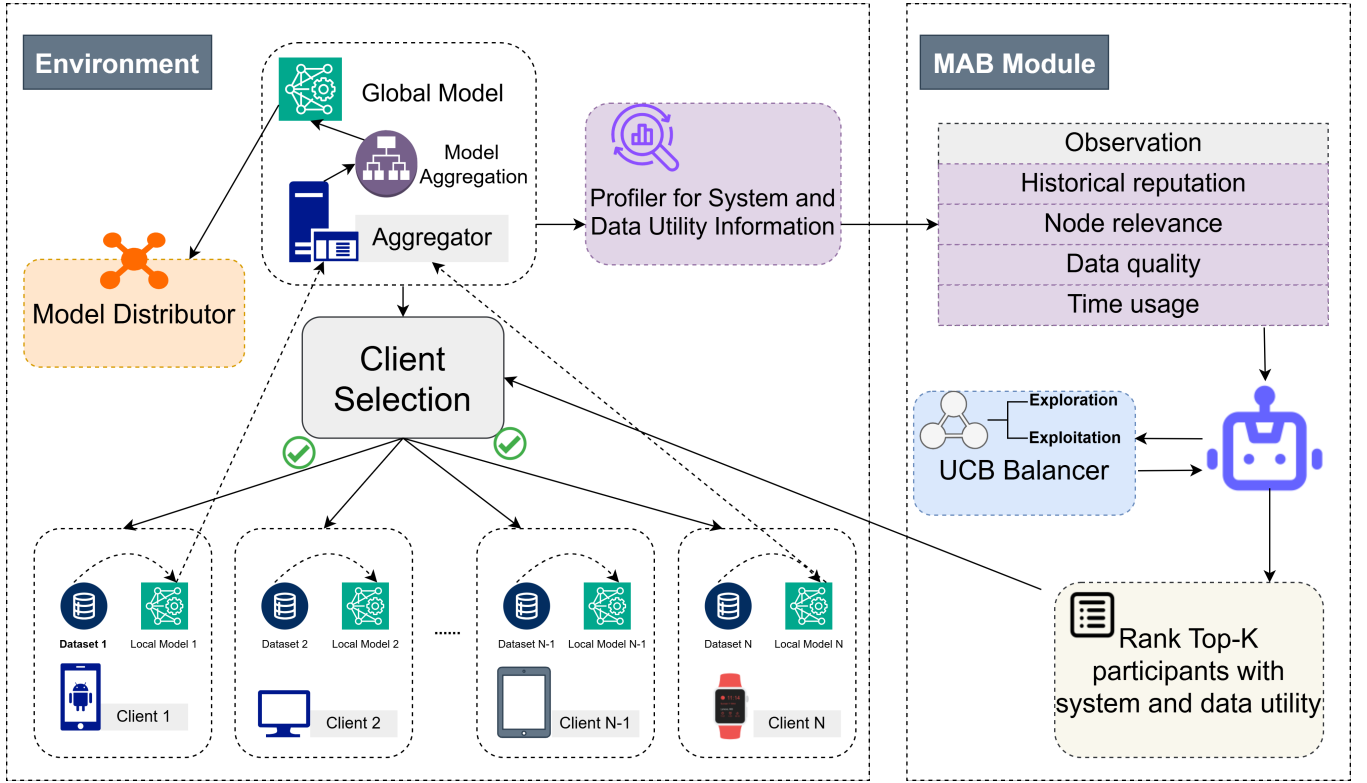


Fig. 2: Framework of the UCB-based MAB for FRS participant selection.

#### IV. REINFORCEMENT LEARNING FORMULATION

In this section, we cast the participant selection problem in FL as a RL task. First, we employ the MAB framework to evaluate client performance online by constructing Upper Confidence Bounds (UCB), achieving a principled balance between exploration and exploitation. Next, we specify the agent's observation and action spaces by combining per-round client features with binary selection decisions. Finally, we propose a reward function that jointly accounts for model improvement and resource consumption, enabling the agent to adaptively maximize cumulative rewards while addressing system heterogeneity and non-stationarity. This approach preserves theoretical guarantees and allows efficient, scalable scheduling of clients in distributed environments. A visualization of our proposed MAB framework is presented in Figure 2.

##### A. Multi-Armed Bandit

1) *Principled Exploration–Exploitation Trade-off*: The MAB framework establishes a principled mechanism for balancing exploration and exploitation by constructing optimistic UCB [55]. During each communication round  $t$  in FL, the algorithm maintains an empirical estimate  $\hat{\mu}_i(t)$  of each client  $i$ 's expected reward, calculated as the running mean of observed feedback.

To promote exploration, an UCB is added to the estimate:

$$UCB_i(t) = \hat{\mu}_i(t) + \rho \sqrt{\frac{\log t}{N_i(t)}} \quad (17)$$

where  $\rho$  is the exploration coefficient. This formula naturally decays the exploration term as  $N_i(t)$  increases, encouraging balanced behavior between well-performing and under-sampled clients.

2) *Dynamic Policy Updating and Scalability*: At the end of each round, the algorithm updates both the empirical reward and selection counts for the selected participants. Over time, this leads to the gradual shift, but occasional exploration persists due to the non-zero exploration bonus. This algorithm ensures resilience against distributional drift or unexpected performance changes in the client population.

The participant selection is operated by choosing the top- $K$  clients with the highest UCB values:

$$\mathcal{C}_t = \arg \max_{C \subseteq \mathcal{I}, |C|=K} \sum_{i \in C} UCB_i(t) \quad (18)$$

where  $\mathcal{I}$  is the full set of clients and  $K$  is the selection budget per round. This strategy transforms the combinatorial scheduling challenge into a tractable linear-time operation by treating each client as an independent arm.

In a contextual extension, the UCB score can be modified to include feature-based models:

$$UCB_i(t) = \hat{\mu}_i(t, x_i^t) + \rho \sqrt{\frac{\log t}{N_i(t)}} \quad (19)$$

where  $x_i^t$  denotes time-varying contextual features (e.g., bandwidth, latency, model divergence) associated with client  $i$  at time  $t$ .

3) *Adaptation to Non-Stationarity and Regret Minimization*: Classical UCB assumes reward stationarity, but practical FL systems often exhibit non-stationarity. To account for this, two common modifications include:

1. Discounted UCB: applying exponential decay to old rewards:

$$\hat{\mu}_i^{(\gamma)}(t) = \frac{\sum_{s=1}^t \gamma^{t-s} r_i(s) \cdot \mathbb{I}\{i_s = i\}}{\sum_{s=1}^t \gamma^{t-s} \cdot \mathbb{I}\{i_s = i\}}, \quad 0 < \gamma < 1 \quad (20)$$

2. Sliding-window UCB, restricting estimates to a recent window of size  $W$ :

$$\hat{\mu}_i^{(W)}(t) = \frac{1}{|W_i(t)|} \sum_{s \in W_i(t)} r_i(s) \quad (21)$$

where  $W_i(t)$  contains the last  $W$  rounds where client  $i$  was selected.

4) *Resource-Awareness and Real-World Deployment*: The MAB framework supports integration of system-level constraints into the reward function. Let  $r_i(t)$  be redefined as:

$$r_i(t) = \text{Utility}_i(t) - \lambda \cdot \text{Cost}_i(t) \quad (22)$$

where  $\lambda$  is a penalty coefficient,  $\text{Utility}_i(t)$  measures model improvement (e.g., validation loss decrease), and  $\text{Cost}_i(t)$  includes communication or computation cost.

This reweighted reward formulation enables budget-aware selection, crucial for resource-constrained FL. Since MAB operates online and decentralized, each participant maintains only minimal state:

$$\text{State}_i = (N_i(t), \hat{\mu}_i(t)) \quad (23)$$

This avoids constructing or storing full models of the participant environment, enhancing privacy and scalability.

The MAB-based participant selection method combines real-time feedback, lightweight statistical computation, and rigorous performance guarantees. It avoids the rigidity of static scheduling by continuously updating its beliefs and policies in reaction to dynamic client conditions, all while maintaining theoretical robustness and practical efficiency.

### B. Observation and Action Space

To formulate the participant selection problem into a sequential decision-making framework, we model it as a MAB problem. At each communication round  $t$ , an agent observes node-specific features, selects a subset of clients, and receives an immediate reward. Over rounds, the agent learns to balance exploration and exploitation, thereby approximating the optimal batch selection without solving the NP-hard program directly [55], [56].

At the beginning of round  $t$ , the agent observes for each client  $i \in \mathcal{N}$  a feature vector

$$\mathbf{o}_t^i = [R_{t-1}^i, \Delta_t^i, U_t^i, \tilde{D}_i, T_{\text{train}}^i, T_{\text{comm}}^i]^\top, \quad (24)$$

where

- $R_{t-1}^i$  and  $\Delta_t^i = Q_t^i - Q_{t-1}$  are the historic and incremental CPR from (9),
- $U_t^i$  is the update relevance defined in (11),

- $\tilde{D}_i$  is the normalized data-quality score from (12),
- $T_{\text{train}}^i$  is the measured wall-clock training time for client  $i$  at round  $t$ ,
- $T_{\text{comm}}^i = d_i/b_i$  is the communication time, with  $d_i$  the model size and  $b_i$  the measured bandwidth.

Before policy evaluation, each dimension of  $\mathbf{o}_t^i$  is standardized over the current client pool.

In each round of FL, the action corresponds to choosing a subset of nodes (from the total set  $N$ ) to participate. For practical implementation: the action is represented as a binary vector  $a \in \{0, 1\}^{|N|}$ , where  $a_n = 1$  indicates node  $n$  is selected, and  $a_n = 0$  indicates it is not. Additionally, we introduced a stochastic policy that produces a probability for each node being selected, which can be used to balance exploration and exploitation in the selection.

This reduces each sub-decision to a single-arm choice, permitting standard MAB index policies to be applied iteratively.

### C. Reward Design

Immediately after aggregation, the environment returns a scalar reward as defined below:

$$r_t = \sum_{i \in \mathcal{N}_{\text{sel}}} S_t^i - \kappa \frac{\max_{i \in \mathcal{N}_{\text{sel}}} (T_{\text{train}}^i + T_{\text{comm}}^i)}{T_{\text{semi-boundary}}}, \quad (25)$$

where  $S_t^i$  is the aggregate contribution score from (13), and the latency penalty matches (16). This immediate feedback is used to update each pulled arm's estimated value.

The agent seeks to maximize the expected cumulative reward over  $T$  rounds:

$$J(\pi) = \mathbb{E}_\pi \left[ \sum_{t=1}^T r_t \right]. \quad (26)$$

In the UCB policy, each arm  $i$  maintains an estimate  $\hat{\mu}_i$  of its expected reward, as well as a selection count  $n_i$ . Initially  $\hat{\mu}_i$  can be set to zero (or to a prior), and  $n_i = 0$ . Whenever arm  $i$  is selected at time  $t$  and receives reward  $r_t$ , these are updated by

$$\hat{\mu}_i \leftarrow \frac{\hat{\mu}_i n_i + r_t}{n_i + 1}, \quad n_i \leftarrow n_i + 1. \quad (27)$$

Thus  $\hat{\mu}_i$  always equals the empirical mean of all rewards observed from arm  $i$ . This estimate is then combined with an exploration bonus to form the UCB index:

At sub-step  $j$  of round  $t$ , the UCB index is

$$I_i(t) = \hat{\mu}_i + \rho \sqrt{\frac{\ln t}{n_i + 1}}, \quad (28)$$

and the top- $K$  indices are sequentially pulled as described in Algorithm 1.

## V. PERFORMANCE EVALUATION

This section presents the evaluation of our method in terms of training efficiency and recommendation quality, compared against established FL baselines under various system and data heterogeneity settings.

---

**Algorithm 1** MAB-based Participant Selection

---

**Require:** Client set  $N$ , budget  $K$ , UCB parameter  $\rho$

```
1: Initialize  $\hat{\mu}_i \leftarrow 0, n_i \leftarrow 0 \forall i \in N$ 
2: for round  $t = 1, \dots, T$  do
3:   for each  $i \in N$  do
4:      $I_i(t) \leftarrow \hat{\mu}_i + \rho \sqrt{\frac{\ln t}{n_i + 1}}$ 
5:   end for
6:   Select  $N_{\text{sel}}$  by sequentially pulling the top- $K$  arms
7:   Execute FL round with  $N_{\text{sel}}$ , compute  $S_t^i$  and  $\hat{T}_i$ 
8:   for each  $i \in N_{\text{sel}}$  do
9:      $r_i \leftarrow S_t^i - \kappa \hat{T}_i$ 
10:     $n_i \leftarrow n_i + 1$ 
11:     $\hat{\mu}_i \leftarrow \hat{\mu}_i + \frac{r_i - \hat{\mu}_i}{n_i}$ 
12:   end for
13: end for
```

---

### A. System Configuration

To emulate a heterogeneous FL environment, we deployed our experiments across eight clients with varying computational and network capabilities, following settings similar to FLASH-RL [15]. As detailed in Table II, the participating clients exhibit a range of configurations, with CPU frequencies consistently operating at approximately 2245.78 MHz. The cluster includes two tiers of clients: four high-resource nodes each equipped with 8 CPU cores and 16 GB of RAM, and four low-resource nodes each with 2 CPU cores and 4 GB of RAM, and the bandwidth of these clients varies from 1600 Mbps to 2 Mbps. This setup enables the simulation of real-world device heterogeneity typical in FL deployments.

TABLE II: Client Device Specifications

Name	CPU Frequency	Cores	RAM	Bandwidth
Client 1	2245.78 MHz	8	16 GB	1600 Mbps
Client 2	2245.78 MHz	8	16 GB	1600 Mbps
Client 3	2245.78 MHz	8	16 GB	100 Mbps
Client 4	2245.78 MHz	8	16 GB	100 Mbps
Client 5	2245.78 MHz	2	4 GB	6 Mbps
Client 6	2245.78 MHz	2	4 GB	6 Mbps
Client 7	2245.78 MHz	2	4 GB	2 Mbps
Client 8	2245.78 MHz	2	4 GB	2 Mbps

### B. Dataset Configuration

We conduct all experiments on the MovieLens-100K dataset, which contains 100,000 ratings from 943 users on 1,682 items [32]. In addition to numerical ratings, we augmented the dataset with different modalities inspired by RPFL [20], each item is accompanied by one poster image and one plot summary, enabling multimodal analysis.

TABLE III: Statistics of the MovieLens-100K Dataset

Statistic	Value
Number of users	943
Number of items	1,682
Number of pictures	1,682
Number of plot summaries	1,682
Number of interactions	100,000

Inspired by the methodology proposed in RPFL [20], we simulate a realistic and heterogeneous data distribution across  $N$  distributed clients. The MovieLens-100K ratings are partitioned based on a *User Balance Index* (UBI) with both exponential and linear distribution, which quantifies the degree of sample balance among clients in terms of the number of assigned user interactions.

$$\text{UBI} = \frac{\min\{|D_1|, \dots, |D_N|\}}{\max\{|D_1|, \dots, |D_N|\}}, \quad (29)$$

where  $|D_i|$  denotes the number of samples assigned to client  $i$ . A UBI close to 1 indicates an almost uniform split, whereas a UBI near 0 reflects a highly skewed allocation. To ensure comparability, the UBI values are set to 0.1172 and 0.0146, consistent with the settings used in RPFL [20].

We first generate a portion vector  $\mathbf{p} = [p_1, \dots, p_N]$  according to one of these strategies—exponential and linear—such that

$$|D_i| = \lfloor p_i \cdot |D| \rfloor, \quad i = 1, \dots, N, \quad (30)$$

where  $|D| = 100,000$  is the total number of ratings with corresponding modality data.

A visualization of the resulting data distributions under different UBI settings and partitioning methods is presented in Figure 3.

### C. Federated Learning Baselines

To evaluate the effectiveness of our proposed method, we compare it against two representative FL baselines, each reflecting a different strategy for client selection and aggregation:

**FedAvg** [52] is the canonical federated averaging algorithm and serves as a foundational benchmark in FL research. In each communication round, it randomly selects a subset of clients to perform local updates, which are then averaged by the server to update the global model. This approach assumes a homogeneous participation pattern and does not explicitly address statistical heterogeneity or participation constraints.

**RPFL** [20] is a recent method that explicitly accounts for statistical heterogeneity among clients. It employs principal component analysis (PCA) on uploaded gradients to identify clusters of clients with similar data distributions. Based on these clusters, RPFL seeks to maximize the number of participants per round while preserving representativeness in the federated updates, thereby improving both convergence stability and final model performance under non-IID settings.

### D. Results and Discussion

We evaluate each method based on two primary dimensions: efficiency and recommendation quality. Efficiency is assessed by measuring the total wall-clock time required to reach convergence, as well as the time needed to achieve a target AUC score of 0.82, using an approach similar to Feng *et al.* [56]. These metrics reflect the overall speed and computational practicality of each method. Meanwhile, recommendation quality is evaluated using three standard metrics at convergence.



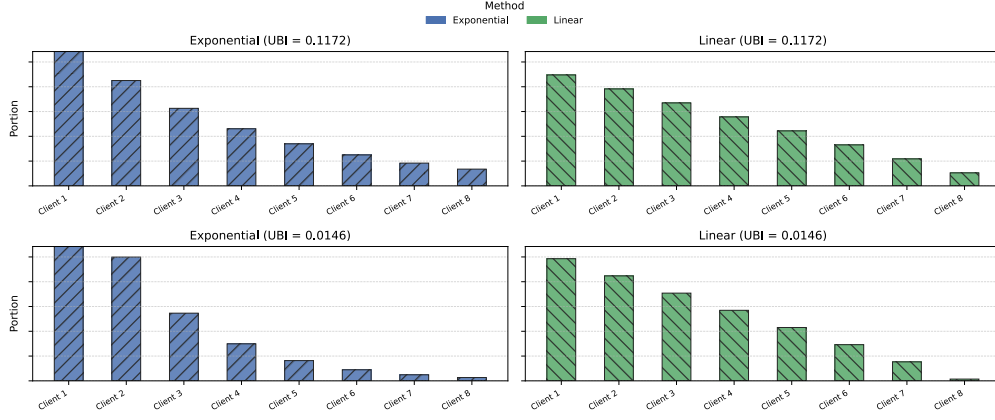


Fig. 3: Allocation of data samples to each client under different UBI settings.

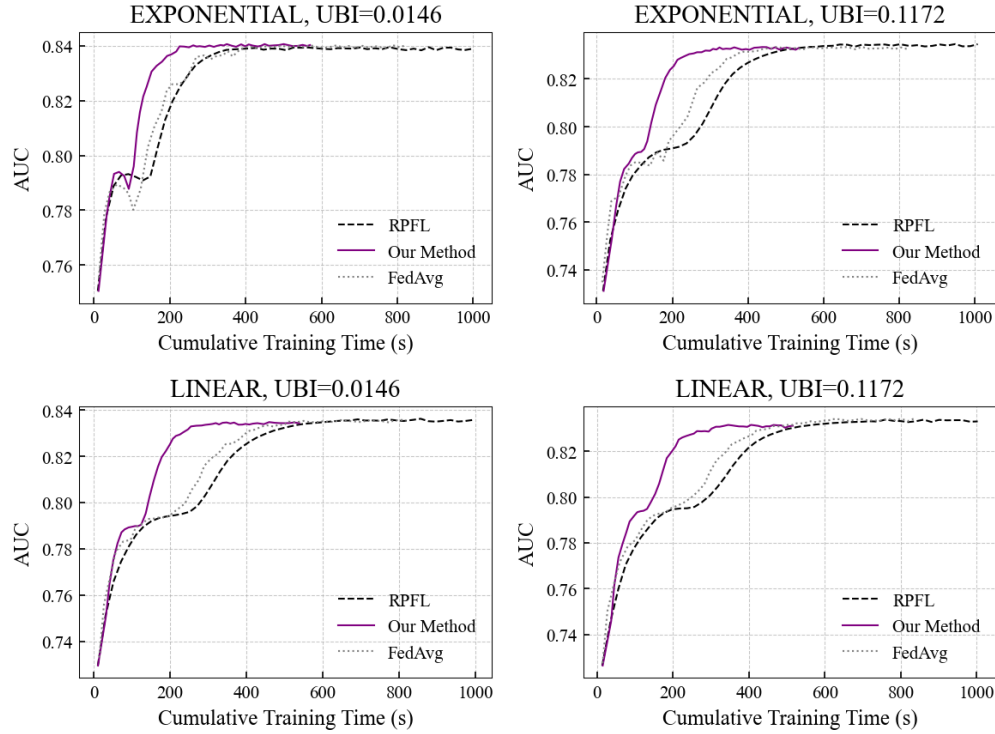


Fig. 4: AUC over training time for RPFL, FedAvg, and our method under exponential and linear partitioning with different UBI settings.

1) *Metrics*: In this work, we use three common metrics to evaluate recommendation quality: Area Under the ROC Curve (AUC), Normalized Discounted Cumulative Gain at rank 50 (NDCG@50), and Recall@50. Together, these metrics capture how well the system ranks relevant items, emphasizes the most important items near the top, and retrieves a high fraction of relevant items in the top-K suggestions.

a) *Area Under the ROC Curve*: AUC measures the probability that a randomly chosen relevant item receives a higher score than a randomly chosen non-relevant item. By plotting the true positive rate against the false positive rate as the decision threshold changes, AUC summarizes the model’s ability to distinguish between relevant and non-

relevant items over all possible thresholds. Values closer to 1.0 indicate better discrimination, while 0.5 corresponds to random ranking.

b) *Normalized Discounted Cumulative Gain at Rank 50*: NDCG@50 evaluates how well the algorithm places truly relevant items within the first 50 positions of the ranked list. It assigns greater importance to higher positions by applying a logarithmic discount to lower ranks, and then normalizes by the best-possible ordering. Thus, NDCG@50 rewards methods that place the most relevant items near the top of the recommendations. Scores range from 0 (poor ordering) to 1 (ideal ordering).

TABLE IV: Performance Comparison under Different Variants and UBI Settings

Distribution	UBI	Method	Total Time (s)	Time to Target (s)	AUC	NDCG@50	Recall@50
Exponential	0.0146	RPFL	1000.568	227.742	0.8387	0.2698	0.2700
		FedAvg	822.532	190.634	0.8395	0.2699	0.2721
		Our Method	570.299	130.408	0.8398	0.2713	0.2796
	0.1172	RPFL	1008.267	359.545	0.8339	0.2711	0.2722
		FedAvg	824.615	303.324	0.8325	0.2615	0.2626
		Our Method	534.102	181.332	0.8326	0.2681	0.2664
Linear	0.0146	RPFL	998.350	373.864	0.8354	0.2674	0.2747
		FedAvg	815.642	323.692	0.8331	0.2628	0.2644
		Our Method	540.834	190.698	0.8340	0.2638	0.2673
	0.1172	RPFL	1003.766	398.802	0.8331	0.2678	0.2806
		FedAvg	828.005	348.800	0.8303	0.2551	0.2702
		Our Method	515.406	206.960	0.8307	0.2585	0.2715

c) *Recall at Rank 50*: Recall@50 computes the fraction of all truly relevant items that appear among the top 50 recommendations. This metric reflects the system’s ability to retrieve as many relevant items as possible within a fixed recommendation budget. Higher Recall@50 means the model covers a larger share of relevant content in its top-K output.

By combining AUC, NDCG@50, and Recall@50, we obtain a balanced view of both global ranking performance and top-K recommendation effectiveness [31].

2) *Performance Overview Across Distributions*: Table IV reports total training time, time to reach AUC = 0.82, and final recommendation metrics for FedAvg, RPFL, and our MAB-based method across four data-distribution scenarios. Overall, our approach delivers substantial end-to-end speedups while matching or slightly improving recommendation quality.

3) *Training Efficiency*: Under both exponential and linear partitions with highly skewed data (UBI = 0.0146), our method reduces total wall-clock time by 30.7%–45.9% compared to FedAvg and by 42.9%–45.9% compared to RPFL. Time to reach the target AUC of 0.82 is cut by 31.6%–41.0%. And when the UBI increases to 0.1172 with more balanced splits, speedups grow even larger: total training time drops by 35.2%–49.0% and time-to-target accelerates by 40.2%–49.5%. These consistent gains across distributions demonstrate that our adaptive selection policy effectively mitigates both data heterogeneity and system-induced delays.

4) *Recommendation Quality*: Despite aggressive acceleration, our method preserves or slightly improves final AUC at convergence. Under UBI = 0.0146, AUC increases by up to 0.0011 over RPFL and by 0.0003 over FedAvg, while NDCG@50 and Recall@50 improve by up to 0.0015 and 0.0096, respectively. For more balanced splits (UBI = 0.1172), AUC differences remain within  $\pm 0.0013$ , and NDCG@50/Recall@50 changes are marginal (within  $\pm 0.0066$  and  $\pm 0.0058$ ). Similar patterns hold under linear partitioning.

These results confirm that our MAB-based sampling does not sacrifice accuracy for speed: by jointly optimizing for data utility and system responsiveness, we match or exceed baseline recommendation performance across all scenarios.

5) *Robustness Across Settings*: Figure 4 illustrates that our method consistently attains steeper AUC-over-time curves across all four data distributions, reaching convergence significantly earlier without plateauing at lower performance. The uniformity of speedups (30%–50%) and negligible variation in quality metrics ( $< 0.0025$  AUC) across UBI values and partitioning strategies underscores the robustness of our approach in heterogeneous federated environments.

## VI. CONCLUSION AND FUTURE WORK

We presented an MAB-driven participant selection framework for FRS that integrates data-quality, system capability, and historical CPR into a unified reward function. Through extensive experiments on MovieLens-100K with multi-modality inputs, our approach consistently accelerates convergence by up to around 50%, while matching or improving final recommendation performance under diverse non-IID settings. This work paves the way for more nuanced, adaptive sampling strategies in heterogeneous FRS deployments.

*Future work*: While our current evaluation provides strong evidence of the benefits of MAB-based selection, several directions remain for broadening and deepening this line of inquiry. First, future work could extend empirical validation to larger and more diverse datasets, enabling an assessment of robustness across richer domains and sparser interaction patterns. Second, integrating differential-privacy noise injection or secure aggregation protocols can create a privacy-enhanced federated recommendation setting, and it should quantify how the privacy-utility trade-off affects convergence speed and personalization quality. Meanwhile, some more advanced DRL techniques can also extend the capability to deal with more complex situation. Lastly, an online meta-learning mechanism could allow the utility-function weights  $\alpha$ ,  $\beta$ , and  $\kappa$  to adjust automatically during training, achieving a dynamic balance among data heterogeneity, communication constraints, and overall system efficiency.

## VII. ETHICS AND DATA PRIVACY

This paper relies solely on the publicly available MovieLens-100K dataset, computer-generated synthetic data,

and theoretical simulations. No human participants were involved, and no personally identifiable or sensitive information was collected, stored, or processed. All datasets used are anonymized and contain no names, contact details, or other privacy details. As such, no ethical approval or data-privacy review was required.

## REFERENCES

- [1] D. Coppola, "Amazon - statistics and facts," Feb. 2025, statista. [Online]. Available: <https://www.statista.com/topics/846/amazon>
- [2] L. Ceci, "Tiktok - statistics & facts," Apr. 2024, statista. [Online]. Available: <https://www.statista.com/topics/6077/tiktok/#topicOverview>
- [3] Q. Zhang, P. Yang, J. Yu, H. Wang, X. He, S.-M. Yiu, and H. Yin, "A survey on point-of-interest recommendation: Models, architectures, and security," *IEEE Transactions on Knowledge and Data Engineering*, vol. 37, no. 6, pp. 3153–3172, 2025.
- [4] J. Yu, H. Yin, X. Xia, T. Chen, J. Li, and Z. Huang, "Self-supervised learning for recommender systems: A survey," *IEEE Transactions on Knowledge and Data Engineering*, vol. 36, no. 1, pp. 335–355, 2024.
- [5] Q. Liu, J. Hu, Y. Xiao, X. Zhao, J. Gao, W. Wang, Q. Li, and J. Tang, "Multimodal recommender systems: A survey," *ACM Comput. Surv.*, sep 2024.
- [6] B. S. Guendouzi, S. Ouchani, H. EL Assaad, and M. EL Zaher, "A systematic review of federated learning: Challenges, aggregation methods, and development tools," *Journal of Network and Computer Applications*, vol. 220, p. 103714, 2023.
- [7] P. Voigt and A. V. dem Bussche, *The EU General Data Protection Regulation (GDPR): A Practical Guide*, 1st ed. Cham: Springer International Publishing, 2017, vol. 10.
- [8] I. Calzada, "Citizens' data privacy in china: The state of the art of the personal information protection law (pipl)," *Smart Cities*, vol. 5, no. 3, pp. 1129–1150, 2022.
- [9] P. Souza, T. Ferreto, and R. Calheiros, "Maintenance operations on cloud, edge, and iot environments: Taxonomy, survey, and research challenges," *ACM Comput. Surv.*, vol. 56, no. 10, jun 2024.
- [10] M. Goudarzi, M. Palaniswami, and R. Buyya, "A distributed deep reinforcement learning technique for application placement in edge and fog computing environments," *IEEE Transactions on Mobile Computing*, vol. 22, no. 5, pp. 2491–2505, 2023.
- [11] M. Goudarzi, Q. Deng, and R. Buyya, *Resource management in edge and fog computing using FogBus2 framework*. United Kingdom: Institution of Engineering and Technology (IET), 2024, pp. 17–52, publisher Copyright: © The Institution of Engineering and Technology 2024.
- [12] M. Ye, X. Fang, B. Du, P. C. Yuen, and D. Tao, "Heterogeneous federated learning: State-of-the-art and research challenges," *ACM Comput. Surv.*, vol. 56, no. 3, oct 2023.
- [13] J. Li, T. Chen, and S. Teng, "A comprehensive survey on client selection strategies in federated learning," *Computer Networks*, vol. 251, p. 110663, 2024.
- [14] Q. Sun, X. Li, J. Zhang, L. Xiong, W. Liu, J. Liu, Z. Qin, and K. Ren, "Shapleyfl: Robust federated learning based on shapley value," in *Proceedings of the 29th ACM SIGKDD Conference on Knowledge Discovery and Data Mining*, ser. KDD '23. New York, NY, USA: Association for Computing Machinery, 2023, p. 2096–2108.
- [15] S. Bouaziz, H. Benmeziane, Y. Imine, L. Hamdad, S. Niar, and H. Ouarnoughi, "Flash-rl: Federated learning addressing system and static heterogeneity using reinforcement learning," in *2023 IEEE 41st International Conference on Computer Design (ICCD)*, 2023, pp. 444–447.
- [16] L. Fu, H. Zhang, G. Gao, M. Zhang, and X. Liu, "Client selection in federated learning: Principles, challenges, and opportunities," *IEEE Internet of Things Journal*, vol. 10, no. 24, pp. 21 811–21 819, 2023.
- [17] M. Goudarzi, M. A. Rodriguez, M. Sarvi, and R. Buyya, "μddrl: A qos-aware distributed deep reinforcement learning technique for service offloading in fog computing environments," *IEEE Transactions on Services Computing*, vol. 17, no. 1, pp. 47–59, 2024.
- [18] Z. Wang, M. Goudarzi, and R. Buyya, "Reinfog: A drl empowered framework for resource management in edge and cloud computing environments," 2024.
- [19] —, "Tf-ddrl: A transformer-enhanced distributed drl technique for scheduling iot applications in edge and cloud computing environments," *IEEE Transactions on Services Computing*, vol. 18, no. 2, pp. 1039–1053, 2025.
- [20] C. Feng, D. Feng, G. Huang, Z. Liu, Z. Wang, and X.-G. Xia, "Robust privacy-preserving recommendation systems driven by multimodal federated learning," *IEEE Transactions on Neural Networks and Learning Systems*, vol. 36, no. 5, pp. 8896–8910, 2025.
- [21] X. Zheng, M. Guan, X. Jia, L. Sun, and Y. Luo, "Federated matrix factorization recommendation based on secret sharing for privacy preserving," *IEEE Transactions on Computational Social Systems*, vol. 11, no. 3, pp. 3525–3535, 2024.
- [22] C. Tian, Y. Xie, X. Chen, Y. Li, and X. Zhao, "Privacy-preserving cross-domain recommendation with federated graph learning," *ACM Trans. Inf. Syst.*, vol. 42, no. 5, May 2024.
- [23] L. Qu, W. Yuan, R. Zheng, L. Cui, Y. Shi, and H. Yin, "Towards personalized privacy: User-governed data contribution for federated recommendation," in *Proceedings of the ACM Web Conference 2024*, ser. WWW '24. New York, NY, USA: Association for Computing Machinery, 2024, p. 3910–3918.
- [24] S. Wang, H. Tao, J. Li, X. Ji, Y. Gao, and M. Gong, "Towards fair and personalized federated recommendation," *Pattern Recognition*, vol. 149, p. 110234, 2024.
- [25] N. Agrawal, A. K. Sirohi, S. Kumar, and J. , "No prejudice! fair federated graph neural networks for personalized recommendation," *Proceedings of the AAAI Conference on Artificial Intelligence*, vol. 38, no. 10, pp. 10 775–10 783, Mar. 2024.
- [26] B. Xie, C. Hu, H. Huang, J. Yu, and H. Xia, "Dci-pfgl: Decentralized cross-institutional personalized federated graph learning for iot service recommendation," *IEEE Internet of Things Journal*, vol. 11, no. 8, pp. 13 837–13 850, 2024.
- [27] Z. Li, X. Wu, W. Pan, Y. Ding, Z. Wu, S. Tan, Q. Xu, Q. Yang, and Z. Ming, "Fedcore: Federated learning for cross-organization recommendation ecosystem," *IEEE Transactions on Knowledge and Data Engineering*, vol. 36, no. 8, pp. 3817–3831, 2024.
- [28] X. Liu, J. Lv, F. Chen, Q. Wei, H. He, and Y. Qian, "Multi-party federated recommendation based on semi-supervised learning," *IEEE Transactions on Big Data*, vol. 10, no. 4, pp. 356–370, 2024.
- [29] X. He, L. Liao, H. Zhang, L. Nie, X. Hu, and T.-S. Chua, "Neural collaborative filtering," in *Proceedings of the 26th International Conference on World Wide Web*, ser. WWW '17. Republic and Canton of Geneva, CHE: International World Wide Web Conferences Steering Committee, 2017, p. 173–182.
- [30] R. He and J. McAuley, "Vbpr: visual bayesian personalized ranking from implicit feedback," in *Proceedings of the Thirtieth AAAI Conference on Artificial Intelligence*, ser. AAAI'16. AAAI Press, 2016, p. 144–150.
- [31] F. Liu, H. Chen, Z. Cheng, A. Liu, L. Nie, and M. Kankanhalli, "Disentangled multimodal representation learning for recommendation," *Trans. Multi.*, vol. 25, p. 7149–7159, Jan. 2023.
- [32] F. M. Harper and J. A. Konstan, "The movielens datasets: History and context," *ACM Trans. Interact. Intell. Syst.*, vol. 5, no. 4, Dec. 2015.
- [33] J. Wen, Z. Zhang, Y. Lan *et al.*, "A survey on federated learning: challenges and applications," *International Journal of Machine Learning and Cybernetics*, vol. 14, pp. 513–535, 2023.
- [34] M. Imran, H. Yin, T. Chen, Q. V. H. Nguyen, A. Zhou, and K. Zheng, "Refs: Resource-efficient federated recommender system for dynamic and diversified user preferences," *ACM Trans. Inf. Syst.*, vol. 41, no. 3, feb 2023.
- [35] Q. Deng, M. Goudarzi, and R. Buyya, "Fogbus2: a lightweight and distributed container-based framework for integration of iot-enabled systems with edge and cloud computing," in *Proceedings of the International Workshop on Big Data in Emergent Distributed Environments*, ser. BiDEDE '21. New York, NY, USA: Association for Computing Machinery, 2021.
- [36] W. Zhu, M. Goudarzi, and R. Buyya, "Flight: A lightweight federated learning framework in edge and fog computing," *Software: Practice and Experience*, vol. 54, no. 5, pp. 813–841, 2024.
- [37] H. Yang, J. Zhao, Z. Xiong, K.-Y. Lam, S. Sun, and L. Xiao, "Privacy-preserving federated learning for uav-enabled networks: Learning-based joint scheduling and resource management," *IEEE Journal on Selected Areas in Communications*, vol. 39, no. 10, pp. 3144–3159, 2021.
- [38] J. Sun, A. Li, L. Duan, S. Alam, X. Deng, X. Guo, H. Wang, M. Gorlatova, M. Zhang, H. Li, and Y. Chen, "Fedsea: A semi-asynchronous

federated learning framework for extremely heterogeneous devices,” in *Proceedings of the 20th ACM Conference on Embedded Networked Sensor Systems*, ser. SenSys ’22. New York, NY, USA: Association for Computing Machinery, 2023, p. 106–119.

- [39] C. Zhang, G. Long, H. Guo, X. Fang, Y. Song, Z. Liu, G. Zhou, Z. Zhang, Y. Liu, and B. Yang, “Federated adaptation for foundation model-based recommendations,” 08 2024, pp. 5453–5461.
- [40] W. Yuan, L. Qu, L. Cui, Y. Tong, X. Zhou, and H. Yin, “Hetefedrec: Federated recommender systems with model heterogeneity,” in *2024 IEEE 40th International Conference on Data Engineering (ICDE)*. Los Alamitos, CA, USA: IEEE Computer Society, may 2024, pp. 1324–1337.
- [41] J. Bian, J. Huang, S. Ji, Y. Liao, X. Li, Q. Wang, J. Zhou, D. Dou, Y. Wang, and H. Xiong, “Feynman: Federated learning-based advertising for ecosystems-oriented mobile apps recommendation,” *IEEE Transactions on Services Computing*, vol. 16, no. 5, pp. 3361–3372, 2023.
- [42] E. Yang, W. Pan, Q. Yang, and Z. Ming, “Discrete federated multi-behavior recommendation for privacy-preserving heterogeneous one-class collaborative filtering,” *ACM Trans. Inf. Syst.*, vol. 42, no. 5, apr 2024.
- [43] Z. Cai, T. Tang, S. Yu, Y. Xiao, and F. Xia, “Marking the pace: A blockchain-enhanced privacy-traceable strategy for federated recommender systems,” *IEEE Internet of Things Journal*, vol. 11, no. 6, pp. 10 384–10 397, 2024.
- [44] X. Ding, G. Li, L. Yuan, L. Zhang, and Q. Rong, “Efficient federated item similarity model for privacy-preserving recommendation,” *Information Processing and Management*, vol. 60, no. 5, p. 103470, 2023.
- [45] Z. Ye, X. Zhang, X. Chen, H. Xiong, and D. Yu, “Adaptive clustering based personalized federated learning framework for next poi recommendation with location noise,” *IEEE Transactions on Knowledge and Data Engineering*, vol. 36, no. 5, pp. 1843–1856, 2024.
- [46] L. Yuan, Z. Wang, L. Sun, P. S. Yu, and C. G. Brinton, “Decentralized federated learning: A survey and perspective,” *IEEE Internet of Things Journal*, pp. 1–1, 2024.
- [47] T. Xia, J. Ren, W. Rao, Q. Zu, W. Wang, S. Chen, and Y. Zhang, “Aerorec: An efficient on-device recommendation framework using federated self-supervised knowledge distillation,” in *IEEE INFOCOM 2024 - IEEE Conference on Computer Communications*, 2024, pp. 121–130.
- [48] Z. Li, G. Long, and T. Zhou, “Federated recommendation with additive personalization,” in *The Twelfth International Conference on Learning Representations*, 2024.
- [49] Z. Li, M. Liu, and J. C. Lui, “Fedconpe: Efficient federated conversational bandits with heterogeneous clients,” in *Proceedings of the Thirty-Third International Joint Conference on Artificial Intelligence*, ser. IJCAI ’24, 2024.
- [50] X. He, S. Liu, J. Keung, and J. He, “Co-clustering for federated recommender system,” in *Proceedings of the ACM Web Conference 2024*, ser. WWW ’24. New York, NY, USA: Association for Computing Machinery, 2024, p. 3821–3832.
- [51] F. Ting, W. Y. Li, and S. X. Qi, “Privacy-enhanced lossless federated recommendation with client-selection,” in *2023 IEEE 29th International Conference on Parallel and Distributed Systems (ICPADS)*, 2023, pp. 2720–2723.
- [52] B. McMahan, E. Moore, D. Ramage, S. Hampson, and B. A. y. Arcas, “Communication-efficient learning of deep networks from decentralized data,” in *Proceedings of the 20th International Conference on Artificial Intelligence and Statistics*. PMLR, Apr. 2017, pp. 1273–1282.
- [53] J. Devlin, M.-W. Chang, K. Lee, and K. Toutanova, “Bert: Pre-training of deep bidirectional transformers for language understanding,” in *Proceedings of the 2019 conference of the North American chapter of the association for computational linguistics: human language technologies, volume 1 (long and short papers)*, 2019, pp. 4171–4186.
- [54] A. Dosovitskiy, L. Beyer, A. Kolesnikov, D. Weissenborn, X. Zhai, T. Unterthiner, M. Dehghani, M. Minderer, G. Heigold, S. Gelly *et al.*, “An image is worth 16x16 words: Transformers for image recognition at scale,” *arXiv preprint arXiv:2010.11929*, 2020.
- [55] E. Boursier and V. Perchet, “A survey on multi-player bandits,” *Journal of Machine Learning Research*, vol. 25, no. 137, pp. 1–45, 2024.
- [56] F. Lai, X. Zhu, H. V. Madhyastha, and M. Chowdhury, “Oort: Efficient federated learning via guided participant selection,” in *15th USENIX*

*Symposium on Operating Systems Design and Implementation (OSDI 21)*. USENIX Association, Jul. 2021, pp. 19–35.